3-D NUMERICAL SIMULATION OF SHEET METAL FORMING PROCESSES USING SOLID ELEMENT

B.K. Chun, J.T. Jinn, and W.T. Wu

Scientific Forming Technologies Corporation, 5038 Reed Road, Columbus, OH 43220, USA

ABSTRACT : This paper addresses two issues in the 3-D numerical simulation of sheet metal forming processes. One is the implementation of an effective solid element on very thin metal sheet under the bending and drawing operations. The other is the use of parallel computational scheme to reduce the simulation time. Possible volumetric and shear locking phenomena for the thin structure with solid element are avoided by adopting the assumed strain concept. Various sheet metal forming processes - square cup drawing process with/without blank holder (NUMISHEET'93 Benchmark) and cylindrical cup drawing process with DDQ steel sheet (NUMISHEET'99 Benchmark) - are simulated with the current implementation. All the results derived from the numerical simulations show good agreement with the corresponding test results. The simulation time can be reduced greatly by utilizing multiple CPUs with the parallelized iterative solver based on the MPI(Message Passing Interface) programming scheme. The scalability of the iterative solver with different configurations is presented in this paper.

1. INTRODUCTION

Among many numerical simulation techniques, the finite element method (FEM) has made significant contributions in the modeling of bulk forming and sheet forming processes in the past decades. DEFORM™-3D is an implicit finite element code. It has been successfully used by the bulk metal forming industry to design and to optimize their forming processes. Hexahedral brick and tetrahedral MINI element formulations are used to account for the large deformation of the bulk material. The current effort is to enhance the code for the sheet forming applications.

Due to advantages in modeling thin structures, the membrane or shell element formulations are very popular in the simulation of sheet forming processes. Although shell elements represent the stress variation through their thickness effectively, they generally require special treatments for the drilling degree of freedom and the transverse shear locking to preserve the Kirchhoff or Reissner-Mindlin hypotheses. Thus, the shell formulation requires more complicated and sophisticated procedures than solid element formulations. Moreover, shell elements do not have the continuity of the thickness over the neighborhood elements. A comprehensive comparison of solid and shell elements can be found in the reference (Wriggers et. al. [1]). In the reference, the authors showed the possibility of the application of solid elements for thin shell as well as thick shell problems.

When dealing with temperature sensitive processes (heat exchange between tooling and the blank, temperature gradient in the thickness direction are expected), or a process with a tailored welded blank that involves multiple thickness sections, the solid element is attractive due to its inherent capability in representing the thickness direction geometrically. In modeling the thin structure, the classical solid elements, however, generally need the additional treatment to avoid volumetric and shear locking phenomena for the thin structure.

In the first part of this paper, the assumed strain solid element will be presented and applied for typical bending and drawing processes. The results are compared with the corresponding experimental measurements. Next, a speed-up technique based on the use of a parallel computational scheme will be presented in this paper.

2. BASIC EQUATIONS

2.1 CONSTITUTIVE EQUATION

The associated flow rule with Hill'48 anisotropic yield criterion (Hill [2]) is used for consideration of initial texture property of sheet metal. The flow potential for orthotropy which conserves three symmetry planes are written in terms of the stress $\boldsymbol{\sigma}$ as,

$$f = \frac{1}{2}\boldsymbol{\sigma}^T \mathbf{P} \boldsymbol{\sigma} - \left(\sigma^o\right)^2 = 0. \qquad (1)$$

with

$$\mathbf{P} = 2\begin{vmatrix} \beta_{11} & -\beta_{12} & -\beta_{13} & 0 & 0 & 0 \\ -\beta_{12} & \beta_{22} & -\beta_{23} & 0 & 0 & 0 \\ -\beta_{13} & -\beta_{23} & \beta_{33} & 0 & 0 & 0 \\ 0 & 0 & 0 & \beta_{44} & 0 & 0 \\ 0 & 0 & 0 & 0 & \beta_{55} & 0 \\ 0 & 0 & 0 & 0 & 0 & \beta_{66} \end{vmatrix} \qquad (2)$$

where $\boldsymbol{\sigma}^T = \{\sigma_{xx}, \sigma_{yy}, \sigma_{zz}, \sigma_{xy}, \sigma_{yz}, \sigma_{xz}\}$ and $\beta_{11} = \beta_{12} + \beta_{13}$; $\beta_{22} = \beta_{12} + \beta_{23}$; $\beta_{33} = \beta_{13} + \beta_{23}$ (or $2\beta_{12} = \beta_{11} + \beta_{22} - \beta_{33}$; $2\beta_{13} = \beta_{11} - \beta_{22} + \beta_{33}$; $2\beta_{23} = -\beta_{11} + \beta_{22} + \beta_{33}$). Therefore, six independent parameters $\beta_{11}, \beta_{22}, \beta_{33}, \beta_{44}, \beta_{55}, \beta_{66}$ need to be defined to characterize the anisotropic hardening state. σ^o is an equivalent stress representing the current yield surface size. The coefficients in **P** can be related to the R-values (Valliappan *et al.* [3]). By setting $\beta_{11} = 1$(this means the principal anisotropic axis coincides the reference axis),

$$\beta_{12} = \frac{R_0}{1+R_0}; \beta_{13} = \frac{1}{1+R_0}; \beta_{23} = \frac{R_0}{R_{90}(1+R_0)};$$
$$\beta_{44} = \frac{(R_0 + R_{90})(1+2R_{45})}{R_{90}(1+R_0)}. \qquad (3)$$

The remaining parameters, β_{55}, β_{66}, can not be determined by the uniaxial tensile test. Generally the corresponding stresses have little effect on sheet metal forming processes, the parameters are assumed to be equal to β_{44}. It should be noted that von-Mises isotropic yield criterion is recovered when three R-values, R_0, R_{45} R_{90} are set to be 1. Numerical implementation of Hill'48 yield criterion is outlined below.

The additive decomposition of strain-rate into elastic and plastic parts is employed together with the normality rule,

$$\dot{\boldsymbol{\varepsilon}} = \dot{\boldsymbol{\varepsilon}}^e + \dot{\boldsymbol{\varepsilon}}^p,$$

$$\dot{\boldsymbol{\sigma}} = \mathbf{C}\dot{\boldsymbol{\varepsilon}}^e,$$

$$\dot{\boldsymbol{\varepsilon}}^p = \dot{\lambda}\left(\frac{\partial f}{\partial \boldsymbol{\sigma}}\right) = \dot{\lambda}\mathbf{a}. \qquad (4)$$

where the superscripts e and p represent the elastic and plastic parts, respectively. **C** is the elasticity tensor, $\dot{\lambda}$ is the plastic strain-rate multiplier and **a** is the flow vector defined by

$$\mathbf{a} = \mathbf{P} \cdot \boldsymbol{\sigma}. \qquad (5)$$

From Equations (4) and (5) with the consistency condition (6), the plastic strain-rate multiplier can be expressed as below:

$$\dot{f} = \frac{\partial f}{\partial \boldsymbol{\sigma}} : \dot{\boldsymbol{\sigma}} + \frac{\partial f}{\partial \sigma^o}\dot{\sigma}^o = 0, \qquad (6)$$

$$\dot{\lambda} = \frac{\mathbf{a}^T \mathbf{C} \dot{\boldsymbol{\varepsilon}}}{\mathbf{a}^T \mathbf{C} \mathbf{a} + A_{iso}}. \qquad (7)$$

where $A_{iso} = 2\sigma^o H \dot{\bar{\varepsilon}}^p$.

Finally, the rate form of the constitutive equation can be written as,

$$\dot{\boldsymbol{\sigma}} = \left(\mathbf{C} - \frac{\mathbf{C}\mathbf{a}\mathbf{a}^T\mathbf{C}}{\mathbf{a}^T\mathbf{C}\mathbf{a} + A_{iso}}\right)\dot{\boldsymbol{\varepsilon}} = \mathbf{C}^{ep}\dot{\boldsymbol{\varepsilon}}. \qquad (8)$$

It should be noted that the element stiffness matrix is directly related to the tangent modulus $\mathbf{C}^{ep}$ evaluated at each integration point, which governs the convergence rate of the global iterative scheme. Thus the consistent tangent modulus is essential to keep the quadratic rate of convergence in the Newton-Raphson

scheme (Simo and Taylor [4], Crisfield [5]).

2.2 SOLID ELEMENT FORMULATION FOR THIN STRUCTURES

A locking-free element is essential for the robustness of the finite element method. Several versions of the reduced integration method using hourglass control techniques have made remarkable progress on this issue (Belytschko and Bachrach [6]; Hughes [7]; Belytschko *et al.* [8]). Li[9] and Jetteur[10] proposed a strain field modification to avoid numerical instability. This paper was based on the method proposed by Li [9]. The essential equations for the strain field description can be written as follows.

$$\boldsymbol{\varepsilon} = \boldsymbol{\varepsilon}^{o} + \boldsymbol{\varepsilon}^{h}. \tag{9}$$

where $\boldsymbol{\varepsilon}^{o}$ and $\boldsymbol{\varepsilon}^{h}$ are the constant and the non-constant terms of the displacement gradient respectively. The non-constant terms can cause undesirable locking, volumetric locking or hourglassing. To avoid these undesirable effects, the modified normal strain part, Equation (11), is assumed to be the same as Equation (12) in Equation (10).

$$\boldsymbol{\varepsilon}^{h} = \boldsymbol{\varepsilon}^{n} + \boldsymbol{\varepsilon}^{s} \cong \boldsymbol{\varepsilon}^{d} + \boldsymbol{\varepsilon}^{s}. \tag{10}$$

where

$$\boldsymbol{\varepsilon}^{n} = \left\{u_{1,1}, u_{2,2}, u_{3,3}, 0, 0, 0\right\}, \tag{11}$$

$$\boldsymbol{\varepsilon}^{d} = \left\{\overline{u}_{1,1}, \overline{u}_{2,2}, \overline{u}_{3,3}, 0, 0, 0\right\}, \tag{12}$$

$$\overline{u}_{i,j} = u_{i,j} - \delta_{ij} u_{k,k}/3. \tag{13}$$

Here, the repeated index is used to denote the summation

Possible shear locking in thin-structure analysis can be resolved on the element level by adopting the the assumed transverse shear strain field (Sze and Yao [11]; Kinkel *et al.* [12]). The transverse shear strains are interpolated from the values evaluated at the mid-points of the element edges as below.

$$\begin{aligned} \widehat{\gamma}_{\varsigma\xi} &= \frac{1-\eta}{2}\gamma_{\varsigma\xi}\Big|_{\xi=0,\eta=-1} + \frac{1+\eta}{2}\gamma_{\varsigma\xi}\Big|_{\xi=0,\eta=+1}, \\ \widehat{\gamma}_{\eta\xi} &= \frac{1-\xi}{2}\gamma_{\eta\varsigma}\Big|_{\xi=-1,\eta=0} + \frac{1+\xi}{2}\gamma_{\eta\varsigma}\Big|_{\xi=+1,\eta=0}. \end{aligned} \tag{14}$$

Several numerical examples will be discussed in the following sections.

3. NUMERICAL EXAMPLES

3.1 NUMISHEET'93 BENCHMARK TEST

This example is taken from the NUMISHEET'93 Benchmark Test[13]. An elasto-plastic material with the von-Mises yield criterion and an isotropic hardening model was used for this example. The material and process data were provided by the committee of NUMISHEET'93. The typical parameters for this simulation are summarized below:

- Blank size: 150 X 150 mm^2
- Blank thickness: 0.81 mm
- Material: Aluminum alloy
  - $\overline{\sigma} = 570.40\,(0.01502 + \overline{\varepsilon}^{p})^{0.3469}$
  - E=70Gpa, v=0.3
- Constant BHF: 19.6 kN
- Punch stroke: 15 mm and 40 mm

The deformed shape at 40mm punch stroke is shown in Figure 1 and the amount of draw-in along the rolling (DX), transverse (DY), and diagonal (DD) directions is compared with the average values of the measurements in Table 1. Since an isotropic yield criterion was used for this simulation, the predicted draw-in along two directions, DX and DY are almost identical in the simulation. Numerical results are well correlated with the measurement results.

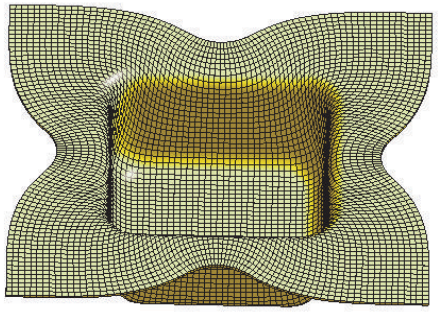

Figure 1 Deformed shape in square cup drawing (aluminum alloy sheet, at 40 mm punch stroke)

Table 1. Draw-in distance

Measured point	Measured	Simulation
15* (DX,DY)	5.3 mm	5.5mm
15*(DD)	3.3 mm	3.3mm
40**(DX,DY)	28.5mm	26.9mm
40**(DD)	15.0mm	15.5 mm

Note) * and ** denotes 15mm , 40mm punch stroke respectively

3.2 CUP INDENTATION PROBLEM

Kawka and Makinouchi [14] and other researchers have shown similar processes as NUMISHET'93 benchmark test, but without a blank holder, to verify their element formulation including the thickness integration and to investigate the wrinkling mode at flange. Except the removing blank holder, the same tooling and process data in section 3.1 have been used for this simulation. (See Figure 2)

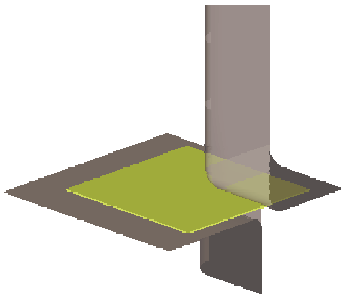

Figure 2 FE model for square cup indentation

The blank is an aluminum alloy sheet with 0.78 mm thickness. The corresponding test results, carried out at Kangwon National University are compared with numerical results in Figure 2. Up to 25 mm of punch stroke, the numerical results have good agreements with the test. Moreover, the folding of the flange can be predicted from the simulation with 30 mm of punch stroke (See Figure 3(c)) (Unfortunately, the corresponding test result is not available).

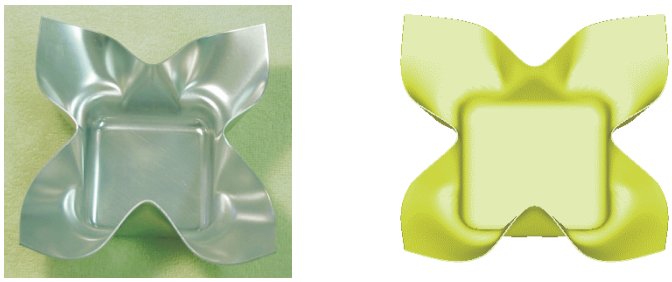

(a) Punch stroke = 20 mm

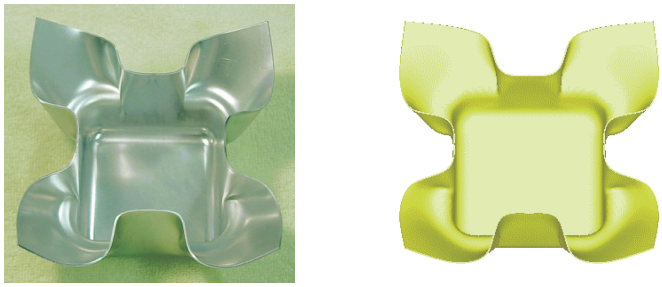

(b) Punch stroke = 25 mm

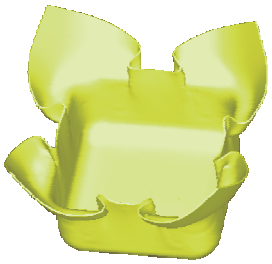

(c) Punch stroke = 30 mm

Fig. 3 Deformed modes in square cup drawing

3.3 NUMISHEET'99 BENCHMARK TEST

This benchmark problem was proposed for NUMISHEET'99 (Benchmark B1-part 2), designed to explore the anisotropic aspects of sheet metal forming processes, both from experiments and numerical simulations [15]. Part I, which is omitted in this paper, refers to a deep drawn cylindrical cup with a hemispherical punch free of any localized necking or

split according to the actual individual forming-limit curve. Part 2 is simulated under given a constant blank holder condition.

The typical parameters for this simulation are summarized below:

- Blank thickness: 1.0 mm
- Drawing ratio: 2.0
- Constant BHF: 80 kN
- Drawing depth : 85 mm
- Material : DDQ (mild steel)
- R-values: $R_0 = 1.73; R_{45} = 1.23; R_{90} = 2.02$

The NUMISHEET'99 committee supplied tool geometries and material data for DDQ(mild steel). The FE model for this benchmark is shown in Figure 4. An elasto-plastic material with the planar anisotropic yield criterion (Hill'48). The earing shapes can be obtained from planar anisotropic yield criterion and the corresponding punch travel and punch force are compared in Figure 5. The amount of draw-in along the rolling (DX), transverse (DY), and diagonal (DD) directions are compared with the measurements in Table 2. The measured data is average values of three participations (B1E-02, B1E-03 and B1E-04) in NUMESHEET'99 benchmark test.

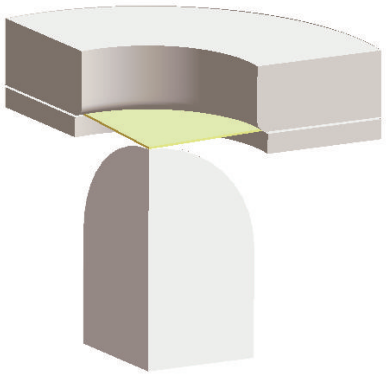

Figure 4 FE model for cylindrical cup drawing

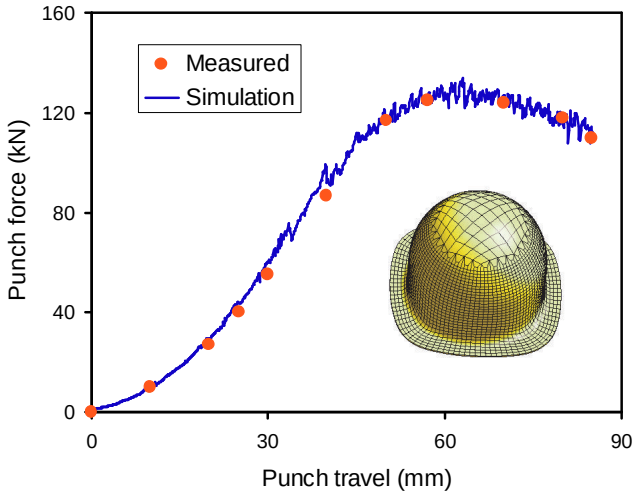

Figure 5 Punch force vs. stroke curve

Table 2. Draw-in distance

Measured point	Measured	Simulation
DX	29.0 mm	27.0 mm
DD	32.0 mm	35.0 mm
DY	27.5 mm	25.0 mm

4. SPEED-UP TECHNIQUES

The rapid advance in computer technologies during last several decades makes 3-D FE models viable for the metal forming applications. However, industry demands have also increased: larger FEM models, more complex shapes, and shorter simulation times. Thus, the development of an efficient solution method has also been one of the thrust areas in the software development.

Generally speaking, the most computationally demanding tasks of an implicit FEM code in solving contact problem are (a) equation solving, (b) contact searching, and (c) stiffness matrix generation. The relative percentage of time spent on these three areas is largely dependent upon the blank mesh size and tool model size. Generally, for a reasonably large industrial problem, the solution solving using a conventional direct solver can take more than 90% of the computing time. Therefore, special attention is being made to speed up the solving procedure.

In order to fully utilize the parallel computing environment, a pre-conditioned conjugate gradient iterative solver was first developed (SFTC [16]) to

replace the direct solver, which solves a set of linear algebraic equations iteratively. The iterative solver was then further developed to use the MPI (Message Passing Interface) facility. The equation solving process using the iterative solver can be carried out not only for multiple CPUs in a single machine, but also for clustering of multiple machines. To compare the performances of MPI implementation, different configurations are employed (SFTC [17]) and the scalability of the iterative solver using MPI with a typical metal forming problem is shown in Table 3. It should be noted that the number of equilibrium iterations was different depending on the number of processors due to the truncation error inherent to parallel computation, however the solutions are almost same. Moreover the scalability appears linear in this example. However, linear scalability can be maintained only under the condition where the balanced network speed and the CPU speed are comparable. Thus continuing to develop the intelligent solution method which can handle with a big size of matrix efficiently, is also requires for fast analysis of 3-D metal forming simulations.

Table 3 Scalability of iterative solver with MPI

Node* (CPU/Node)	Scalability	
	100 Mb Ethenet	1Gb Myrinet
1*1	1.0	
1*2	2.20	2.20
2*1	2.48	2.57
1*4	2.94	2.60
2*2	3.49	3.64
4*1	3.84	4.39
2*3	2.67	3.34
3*2	4.87	5.33
6*1	5.09	6.33

Note) Processor : Intel PIII 55 MHz(512 KB Cache)
Network: 100 Mb Ethenet and 1Gb Myrinet

5. CONCLUSIONS

In order to provide a robust and fast solution method for 3-D sheet metal forming process, two issues are discussed in this paper. One is the use of solid element with the assumed strain and the other is speed-up technique with MPI programming. For typical 3-D sheet metal forming processes, square cup drawing, square cup indentation and cylindrical cup drawing, a good agreement with the corresponding test results is obtained. The improvement in simulation time with the MPI implementation is also presented. It is believed that the current development, use of multiple CPU based on MPI programming, is one of the efficient ways in the 3-D sheet metal forming simulation.

ACKNOWLEDGEMENTS

The authors would like to express sincere gratitude to : Professor H.Y.Kim for providing the cup indentation test data; Mr. Jeffrey Fluhrer for proofreading the manuscript.

REFERENCES

[1] Wriggers, P.,Eberlein, R., and REESE, S., 1996, A comparison of three-dimensional continuum and shell elements for finite plasticity, Int. J. Solids Str., 33(20-22), pp.3309-3326

[2] Hill, R., 1950, The Mathematical Theory of Plasticity, Oxford Univ. Press, London, Chapter 12

[3] Valliappan, S., Boonlaulohr, P., and Lee, I. K., 1976, Non-linear analysis for anisotropic materiala, Int J Num Meth Eng. 10, 597-606.

[4] Simo, J.C. and Taylor, R.L., 1985, Consistent tangent operators for rate independent elasto-plasticity, Comp. Meth. Appl. Mech. Eng., 48, pp. 101-118

[5] Crisfield,M.A., 1987, Consistent schemes for plasticity computation with the Newton-Raphson method, Computational plasticity, part I, pp. 133-159

[6] Belytschko, T. and Bachrach. W.E., 1986, Efficient implementation of quadrilaterals with high coarse-mesh accuracy, Comp. Meth. Appl. Mech. Eng., 54, pp. 279-301

[7] Hughes, T.J.R., 1980, Genralization of selective integration procedures to anisotropic and nonlinear media, Int. J. Num. Meth. Eng., 15, pp. 1413-1418

[8] Belytschko, T., Ong. J.S., Liu, W.K. and Kennedy, J.M., 1984, Hourglass control in linear and nonlinear problems, Comp. Meth. Appl. Mech. Eng., 43, pp. 251-276

[9] Kaiping Li, 1995, Contribution to the finite element simulation of three-dimensional sheet metal forming, Ph.D thesis, MSM, Universite de Liege, Belgique

[10] Jetteur, P., 1991, A mixed finite element for the analysis of large inelastic strains, Int. J. Num. Meth. Eng., 13, pp. 229-239

[11] Sze, KY, and Yao, LQ, 2000, A hybrid stress ANS solid-shell element and its generalization for smart structure modeling. Part I-solid-shell element formulation, International Journal for Numerical Methods in Engineering, 48, pp. 545-564

[12] Kinkel, S, Gruttmann, F, Wagner, W, 1999, A continuum based three-dimensional shell element for laminated structures, Computers and Structures, 71, pp. 43-62

[13] Makinouchi, A., Nakamachi, E., Onate, E., and Wagoner, R.H. (Eds.), 1993, Proceeding of the 2nd International Conference - NUMISHEET'93, Isehara, Japan

[14] Kawka, M. and Makinouchi, A., 1993, Shell element formulation in the static explicit FEM code for simulation of sheet stamping, Proceedings of NUMISHEET'93, pp97-107

[15] Gelin, J. C. and Picart, P., 1999, Proceedings of NUMISHEET'99 - The 4th international conference and workshop on numerical simulation of 3D sheet forming processes, France, September 13-17.

[16] SFTC, 2000, Handout of DEFORM Users group meeting, Columbus, Ohio, USA, May 9-10

[17] SFTC, 2001, Handout of DEFORM Users group meeting, Columbus, Ohio, USA, May 1-2